

# RSC Advances



This is an *Accepted Manuscript*, which has been through the Royal Society of Chemistry peer review process and has been accepted for publication.

*Accepted Manuscripts* are published online shortly after acceptance, before technical editing, formatting and proof reading. Using this free service, authors can make their results available to the community, in citable form, before we publish the edited article. This *Accepted Manuscript* will be replaced by the edited, formatted and paginated article as soon as this is available.

You can find more information about *Accepted Manuscripts* in the [Information for Authors](#).

Please note that technical editing may introduce minor changes to the text and/or graphics, which may alter content. The journal's standard [Terms & Conditions](#) and the [Ethical guidelines](#) still apply. In no event shall the Royal Society of Chemistry be held responsible for any errors or omissions in this *Accepted Manuscript* or any consequences arising from the use of any information it contains.



Journal Name

ARTICLE

## Enhancing the visible-light-induced photocatalytic activity of $\text{AgNbO}_3$ by loading Ag @ AgCl nanoparticles

Leifei Yang, Junbo Liu\*, Haibo Chang\* and Shanshan Tang

New visible-light-driven plasmonic photocatalyst  $\text{Ag@AgCl/AgNbO}_3$  is prepared via loading with  $\text{Ag@AgCl}$  nanoparticles by an impregnating precipitation photoreduction method. The physical and chemical properties of catalysts are characterized by X-ray diffraction, X-ray photoelectron spectroscopy, scanning electron microscope and UV-Visible diffuse reflectance spectra. In comparison with pristine  $\text{AgNbO}_3$ ,  $\text{Ag@AgCl/AgNbO}_3$  exhibits a highly visible-light-induced photocatalytic activity for degradation of methylene blue. Moreover, the photocatalytic mechanism is also discussed. The photoexcited electrons on the surface of the silver nanoparticles are injected due to surface plasmon resonance, and formed radical groups ( $\text{O}_2^-$ ,  $\cdot\text{HOO}$ ,  $\cdot\text{OH}$  and  $\text{Cl}^0$ ), which enhance the photocatalytic activity of  $\text{Ag@AgCl/AgNbO}_3$  in visible-light.

### Introduction

Nowadays, the development of photocatalysts with visible-light response has been studied extensively from the viewpoint of the utilization of solar light energy. Semiconductor photocatalysis has attracted a great deal of attention as a useful technique of water splitting and decontamination treatment in polluted water.<sup>1,2</sup> Silver niobate,  $\text{AgNbO}_3$  with a perovskite structure is a multifunctional material with extensive application potential in photocatalysis, microwave communications and microelectronic technology.<sup>3-5</sup> With a band gap of 2.8 eV,  $\text{AgNbO}_3$  absorbs well into the visible spectrum and has shown significant visible-light activity for  $\text{O}_2$  evolution from an aqueous silver nitrate solution, which acts as the oxidizing agent.<sup>6</sup> However, pristine  $\text{AgNbO}_3$  photocatalytic activity for decomposition of organic pollutants is low. Therefore, much progress has been made to improve the photocatalytic activity by doping metal ions and metal oxides on the surface of  $\text{AgNbO}_3$ .<sup>7-9</sup>

In particular, photocatalysts modified with noble metals like Au and Ag have received more and more attentions.<sup>10-13</sup> Noble metal exhibits unique optical properties due to the surface plasmon resonance (SPR). Zhou *et al.* showed<sup>14</sup> that  $\text{TiO}_2$  film modified by Ag can significantly enhance the visible-light photocatalytic activity. Because the SPR can dramatically amplify the absorption of visible-light. And Zhou *et al.* also reported microwave hydrothermal preparation and visible-light photoactivity of plasmonic photocatalyst Ag- $\text{TiO}_2$  nanocomposite hollow spheres.<sup>15</sup> Moreover, high efficient plasmonic photocatalysts Ag/AgX have been developed and have aroused broad interest.<sup>16-20</sup> Wang *et al.* reported Ag@AgCl, Ag@AgBr and Ag@AgCl-AgI plasmonic photocatalysts, which have been prepared by an ion-exchange method and light-induced reaction.<sup>21-23</sup> Wang *et al.* indicated that AgBr/ $\text{AgNbO}_3$  photocatalytic activity was greatly enhanced in comparison with pure  $\text{AgNbO}_3$ .<sup>24</sup>

Normally,  $\text{AgNbO}_3$  particles were prepared by traditional high-

\*College of Resource and Environmental Science, Jilin Agricultural University, Changchun 130118, Jilin Province, China. E-mail: liujb@mail.ccit.edu.cn. (Junbo Liu). Fax: +86-0431-84532955

\*College of Resource and Environmental Science, Jilin Agricultural University, Changchun 130118, Jilin Province, China. E-mail: jlchhb@163.com. (Haibo Chang). Fax: +86-0431-84532955

temperature solid-state reaction, which require calcination of oxide and nitrate precursors at temperatures in excess of 900 °C with frequent grindings.<sup>25</sup> Soft chemical methods, such as the use of sol-gel precursors or molten salts as reaction media, have been adopted for the synthesis of oxide, but these methods involve often complex operating procedures.<sup>7</sup> The mild hydrothermal method is an attractive route to prepare the inorganic solids due to the relatively mild conditions, one step synthetic procedure and controllable particle size distribution.<sup>26,27</sup>

In this work, we have successfully synthesized AgNbO<sub>3</sub> particles by hydrothermal method. Ag@AgCl/AgNbO<sub>3</sub> photocatalyst was synthesized by depositing AgCl nanoparticles on the AgNbO<sub>3</sub> powders and then reducing partial Ag<sup>+</sup> ions in the AgCl particles to Ag<sup>0</sup> species under xenon lamp irradiation. The visible-light photocatalytic activity of prepared samples was measured by photocatalytic degradation of methylene blue (MB), and the mechanism has been discussed.

## Results and discussion

### Catalyst characterization

XRD was used to determine the phase structure of the AgNbO<sub>3</sub> and Ag@AgCl/AgNbO<sub>3</sub>. Fig. 1a is the XRD pattern of AgNbO<sub>3</sub>, which indicates perovskite-type diffraction patterns. All peaks in the pattern can be indexed using AgNbO<sub>3</sub> perovskite structure (JCPDS Card No: 52-0405) and their corresponding crystalline planes were marked. No characteristic peaks belonging to other impurities were detected, which indicated that pure precursors had been synthesized. The XRD patterns of Ag@AgCl/AgNbO<sub>3</sub> (AgNO<sub>3</sub> concentrations is 0.5 M-2.0 M) showed that, in comparison with Fig. 1a, new strong diffraction peaks appear at the positions about 27.8°, 55.1° and 74.6°, corresponding to (111), (311) and (331) diffraction peaks of AgCl (JCPDS Card No: 85-1355), which are marked with ▽ in the Fig. 1(b-g). The diffraction peaks of AgCl appear in Fig. 1(b-g) due to the following chemical reaction (1). Ag atoms produced via photochemical or photocatalytic reduction reaction of AgCl under xenon lamp light in the presence of AgNbO<sub>3</sub> by formula (2). Ag atoms aggregated to form small silver nanocrystals, and deposited on the surface of AgCl particles.<sup>28</sup> However, there are no the diffraction peaks of metallic Ag in Fig.

1(b-g), because a small amount of Ag nanoparticles have deposited on the surface of AgNbO<sub>3</sub> below the detection limit of XRD analysis.

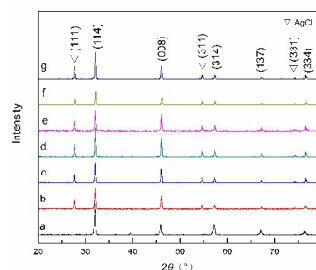
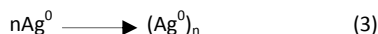
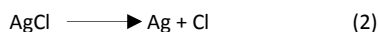
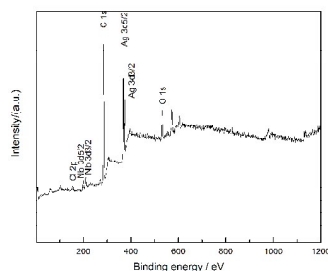


**Fig. 1** XRD patterns of AgNbO<sub>3</sub> (a) and Ag@AgCl/AgNbO<sub>3</sub> (b-g) obtained in the presence of AgNO<sub>3</sub>: (b) 0.5 M, (c) 1.0 M, (d) 1.25 M, (e) 1.5 M, (f) 1.75 M, (g) 2.0 M.

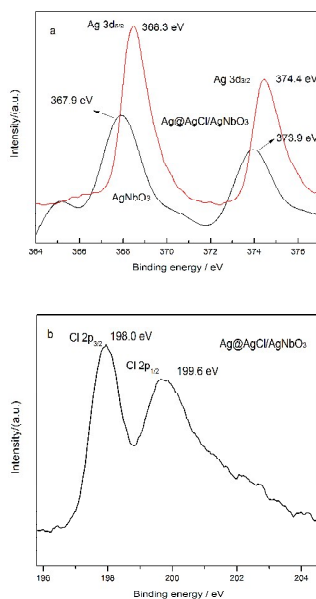
The surface element composition and chemical state of AgNbO<sub>3</sub> and Ag@AgCl were further analyzed by X-ray photoelectron spectroscopy. Fig. 2 shows the XPS spectrum of the Ag, Nb, O, C and Cl peak regions in the Ag@AgCl/AgNbO<sub>3</sub> (AgNO<sub>3</sub> concentration is 1.5 M) in a wide energy range. The C contamination was probably connected with long time exposure to atmosphere or the adventitious hydrocarbon from the XPS instrument itself. The Cl obviously appeared in the spectra of Cl 2p peak, showing the AgCl was successfully modified on the surface of AgNbO<sub>3</sub>, which is in accordance with the XRD analysis.

Fig. 3(a) shows the XPS spectra of the Ag peak regions in the AgNbO<sub>3</sub> and Ag@AgCl/AgNbO<sub>3</sub> (AgNO<sub>3</sub> concentration is 1.5 M). As it is clearly seen the Ag 3d spectra consist of two peaks corresponding to their angular momentum of electrons. Ag 3d<sub>3/2</sub> and Ag 3d<sub>5/2</sub> peaks were identified at 374.4 eV and 368.3 eV in Ag@AgCl/AgNbO<sub>3</sub>, respectively. The difference of two peaks is 6.1 eV from binding energy, which reveals that the silver is of partial metallic nature on the surface of AgNbO<sub>3</sub>.<sup>28,29</sup> Zhang *et al.*<sup>30</sup> also have reported that the peaks at 374.3 eV and 368.6 eV can be attributed to Ag<sup>0</sup>, whereas the peaks at 367.7 eV and 373.7 eV can be attributed to Ag<sup>+</sup>. The Fig. 3(b) shows the XPS spectrum of the Cl

peak regions in the Ag@AgCl /AgNbO<sub>3</sub>. Two peaks at 199.6 eV and 198.0 eV appear in the Cl 2p spectrum, corresponding to the binding energies of Cl 2p<sub>1/2</sub> and Cl 2p<sub>3/2</sub>, respectively, with a doublet separation of 1.6 eV.<sup>24</sup>

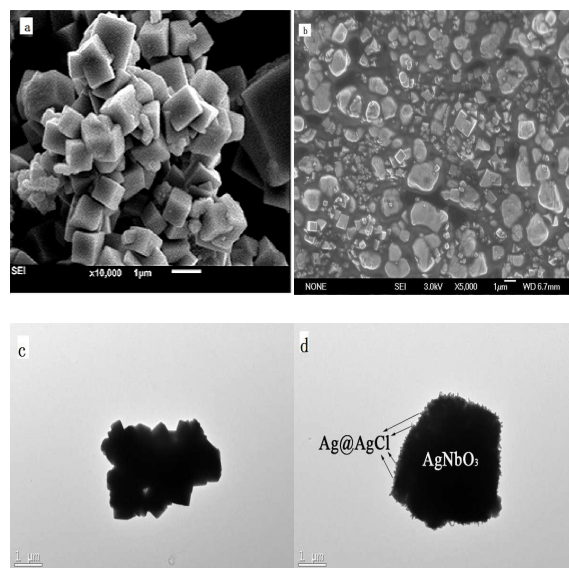


**Fig. 2** XPS survey spectrum of Ag@AgCl/AgNbO<sub>3</sub> obtained in the presence of AgNO<sub>3</sub>: 1.5 M.



**Fig. 3** XPS spectra of AgNbO<sub>3</sub> and Ag@AgCl/AgNbO<sub>3</sub>: (a) Ag, (b) Cl.

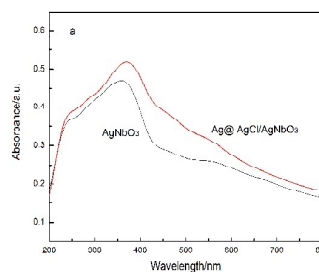
Fig. 4 shows typical SEM images of the as-prepared AgNbO<sub>3</sub> and Ag@AgCl/AgNbO<sub>3</sub> (AgNO<sub>3</sub> concentration is 1.5 M) particles. From Fig. 4(a), it can be found that the cube AgNbO<sub>3</sub> aggregated, and particle size is larger than 1 μm. Fig. 4(b) displays the SEM image of Ag@AgCl/AgNbO<sub>3</sub> after the precipitation and reduction process. The aggregates particles were broken and dispersed by the ultrasound. The particle size obviously decreases. Fig. 4(c) is TEM image of pure AgNbO<sub>3</sub> particles. Fig. 4(d) is TEM image of Ag@AgCl/AgNbO<sub>3</sub> particles (AgNO<sub>3</sub> concentration is 1.5 M), whose surfaces have been covered obviously with a large number of Ag@AgCl particles.



**Fig. 4** SEM and TEM images of AgNbO<sub>3</sub> (a, c) and Ag@AgCl/AgNbO<sub>3</sub> (b, d).

To investigate the optical properties of the AgNbO<sub>3</sub> and Ag@AgCl/AgNbO<sub>3</sub>, the samples were analyzed by diffuse reflectance spectra. As illustrated in Fig. 5(a), each of the samples absorbs well in the visible spectrum. Compared with pure AgNbO<sub>3</sub> whose wave absorption edge is about 510 nm, the absorption threshold edge of Ag@AgCl/AgNbO<sub>3</sub> (AgNO<sub>3</sub> concentration is 1.5 M) is about 590 nm. Because the AgCl was irradiated under xenon lamp to get partial Ag<sup>0</sup> nanoparticles on the surface of AgCl particles. This photocatalyst exhibited a high photocatalytic activity and good stability under visible light irradiation owing to SPR absorption by Ag nanoparticles and the efficient charge separation at the Ag nanoparticles.<sup>31-33</sup>

The optical band gap  $E_g$  of a semiconductor could be deduced according to the following equation  $(Ah\nu)^2 = h\nu - E_g$ , where  $A$  means the absorption coefficient,  $h$  is planck's constant,  $\nu$  is the incident photon frequency, and  $E_g$  is the band gap. Fig. 5(b) showed the  $E_g$  of AgNbO<sub>3</sub> was elicited to be 2.75 eV, and  $E_g$  of Ag@AgCl/AgNbO<sub>3</sub> (AgNO<sub>3</sub> concentration is 1.5 M) was found to be 2.55 eV. This result indicated that doped Ag@AgCl nanoparticles on the surface of AgNbO<sub>3</sub> could narrow the band gap of catalysts, which might be conducive to improve the photocatalytic activity of the composite.



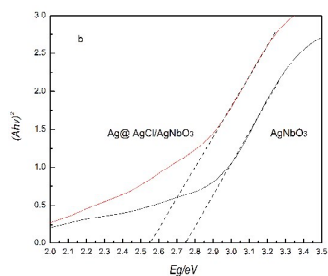


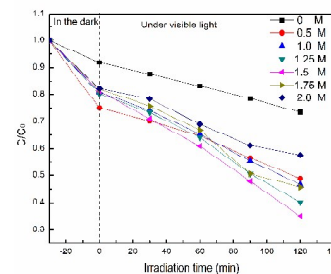
**Fig. 5** (a) UV-Vis DRS spectra for  $\text{AgNbO}_3$  and  $\text{Ag@AgCl/AgNbO}_3$  obtained in the presence of  $\text{AgNO}_3$ : 1.5 M; (b) band gap of photocatalysts.

The photocatalytic activity of the samples were evaluated by photocatalytic degradation decolorization of methylene blue (MB) aqueous solution under visible-light irradiation. Pure  $\text{AgNbO}_3$  and  $\text{Ag@AgCl/AgNbO}_3$  were chosen as the reference photocatalysts for comparison. The photocatalytic results are shown in Fig. 6, before irradiation, the MB solution containing the catalyst was kept in the dark for 30 min to obtain the adsorption-decolorization equilibrium state. Pure  $\text{AgNbO}_3$  exhibited stronger adsorptive capacities for MB in the dark after 30 min, while as the loading amount of  $\text{Ag@AgCl}$  increased, the adsorption becomes smaller gradually. After 2 h visible-light irradiation, the degradation rate for MB of  $\text{AgNbO}_3$  ( $\text{AgNO}_3$  concentrations was 0) catalyst was only 20.2%. While for  $\text{Ag@AgCl/AgNbO}_3$  ( $\text{AgNO}_3$  concentrations were 0.5 M, 1.0 M, 1.25 M, 1.5 M, 1.75 M and 2.0 M, respectively.), the corresponding degradation rate constant values  $k$  were estimated to be 34.9%, 42.2%, 49.9%, 56.9%, 44.3% and 29.9%, respectively. We can see that when concentration of  $\text{AgNO}_3$  was 1.5 M, the photocatalytic effect was optimum, and the degradation rate of 2 h reached to 56.9%. Compared with the  $\text{AgNbO}_3$  on the degradation rate of MB, it increased by 36.7%. After the loading  $\text{Ag@AgCl}$  nanoparticles on the surface of  $\text{AgNbO}_3$ , the optical response of the photocatalyst was extended, which was due to the SPR effect. The photocatalytic activity of the  $\text{Ag@AgCl/AgNbO}_3$  composite was increased observably with the increasing  $\text{AgNO}_3$  content. The photocatalytic activity decreased when  $\text{AgNO}_3$  concentration was over 1.5 M. Mainly because large amounts of  $\text{Ag@AgCl}$  were loaded on the part of active center of  $\text{AgNbO}_3$ , which reduces the reactive group in the solution and decreases photocatalytic performance.

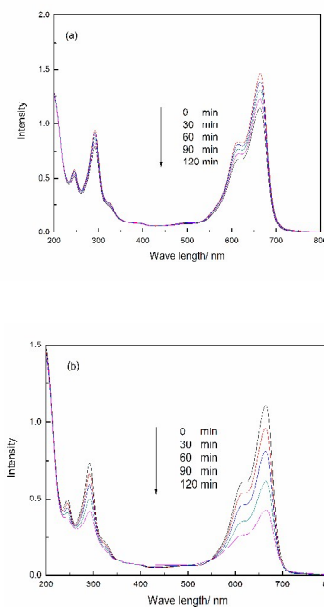
Furthermore, the temporal absorption spectra variation of MB aqueous solution under the visible-light irradiation in the present of  $\text{AgNbO}_3$  and  $\text{Ag@AgCl/AgNbO}_3$  were showed in Fig. 7. It was obviously found that degradation rate for MB of  $\text{Ag@AgCl/AgNbO}_3$  was much higher than that of pure  $\text{AgNbO}_3$ .

Fig. 8 showed that decomposition of MB increases significantly with the increasing of  $\text{AgNO}_3$  concentration from 0 to 2.0 M. It reached a maximum kinetic rate constant at 1.5 M  $\text{AgNO}_3$ , and then decreases with the further increasing of  $\text{AgNO}_3$  concentration. On the basis of the above results and discussion, we concluded that the optimum  $\text{AgNO}_3$  concentration is 1.5 M, which is consistent with the result of photocurrent. The photocatalytic activity of

$\text{Ag@AgCl/AgNbO}_3$  is about 2 times higher than that of pure  $\text{AgNbO}_3$ .



**Fig. 6** Photocatalytic decolorization rate of MB of  $\text{Ag@AgCl/AgNbO}_3$  obtained in the presence of  $\text{AgNO}_3$ : 0M, 0.5M, 1.0M, 1.25M, 1.5M, 1.75M, 2.0M.



**Fig. 7** Absorption spectra changes of MB under visible light irradiation for  $\text{AgNbO}_3$  (a) and  $\text{Ag@AgCl/AgNbO}_3$  (b) obtained in the presence of  $\text{AgNO}_3$ : 1.5 M.

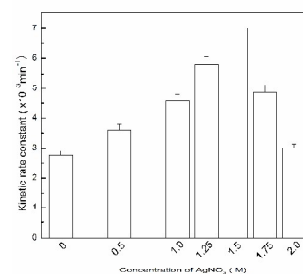


**Fig. 8** Kinetic rate constants for different concentration of  $\text{AgNO}_3$ .

## Photocatalytic mechanism

Under visible light, AgNbO<sub>3</sub> has a certain degree of light absorption. It is well-known that in the photocatalytic process, the electron of the valence band of the AgNbO<sub>3</sub> can be excited when illuminated by light of appropriate wavelength (equal to or greater than the band gap energy). And then the electrons are elevated to the unoccupied conduction band, creating electron-hole pairs which are utilized to initiate redox chemistries with surface absorbed substrates. The electron-hole recombination is the principle reason for the decrease of the photocatalytic efficiency.

Under visible-light irradiation, photo-generated electron-hole pairs are formed in Ag nanoparticles (NPs) due to surface plasmon resonance. The photoexcited electrons at the silver NPs are injected into the AgNbO<sub>3</sub> conduction band (Fig. 9), silver nanoparticles and the injected electrons can be transferred to the ubiquitously present molecular oxygen to form active species O<sub>2</sub><sup>-</sup>, ·HOO, H<sub>2</sub>O<sub>2</sub> and ·OH. Meanwhile, the holes transfer to the surface of the AgCl particles due to the surface of AgCl particles with negatively surface charged. The transferred holes will cause the oxidation of Cl<sup>-</sup> ions to Cl<sup>0</sup> atoms.<sup>16-18</sup> These active species will result in the degradation and mineralization of MB. Thus the Ag NPs can be rapidly regenerated and the Ag@AgCl/AgNbO<sub>3</sub> system remained stable. The major reaction steps in this plasmonic photocatalytic mechanism under visible light irradiation are summarized by eqs (1-9) as follows.<sup>17,19,20</sup>

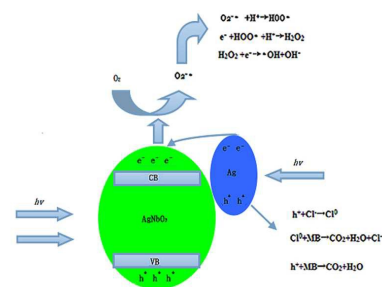
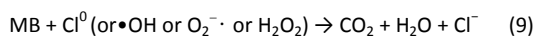
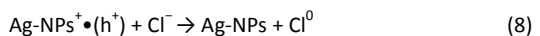
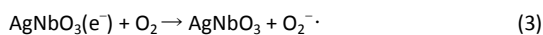
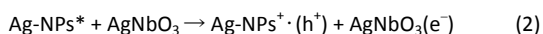


Fig. 9 Photocatalytic mechanism of Ag@AgCl/AgNbO<sub>3</sub> composites.

## Experimental

### 1 Sample preparation

All chemicals used in this study were received from Shanghai Chemical Regent Factory of China. The AgNbO<sub>3</sub> samples were prepared by hydrothermal method, as we reported previously.<sup>34</sup> Ag@AgCl nanoparticles were deposited on the surface of as-synthesized AgNbO<sub>3</sub> powders via an impregnating-precipitation-photoreduction method.<sup>35</sup> The AgNbO<sub>3</sub> powders (0.2 g) were added to 50 mL of deionized water, and the suspension was sonicated for 10 min at room temperature. 10 ml of 0.5-2.0 mol/L AgNO<sub>3</sub> solution and 10 ml 0.5-2.0 mol/L HCl aqueous solution were added and stirred for 20 min, respectively. The mixture were collected by washed with deionized water and dried at 80 °C for 10 h. Finally, the powders were irradiated with the xenon lamp (350 W) for 30 min. They then obtained a dark color, revealing the presence of silver particles.

### 2 Characterizations of the prepared composites

The powder XRD data were collected on a Rigaku D/Max 2500 V/PC X-ray diffractometer (Tokyo, Japan) with CuKα radiation ( $\lambda = 1.5418 \text{ \AA}$ ) at 50 kV and 200 mA at room temperature by step scanning mode in the range  $20^\circ \leq 2\theta \leq 80^\circ$  with increments of  $0.02^\circ$ . X-ray photoelectron spectroscopy (XPS) was performed with a PHI 1600 spectroscope using MgKα X-ray source for excitation. The nanoparticle morphology was measured using a scanning electronic microscope (SEM, JEOL JSM-7001F). UV-vis diffuse reflectance spectra (DRS) were recorded on a UV-vis spectrophotometer (Hitachi U-4100) with BaSO<sub>4</sub> as the reflectance standard material.

### 3 Photocatalytic degradation of MB

For the evaluation of visible-light photocatalytic activity, the 350 W xenon lamp equipped with a UV-cutoff-filter (providing visible-light with  $\geq 400 \text{ nm}$ ) was used as a visible-light source, and the average light intensity striking the surface of the reaction solution was about  $80 \text{ mWcm}^{-2}$ . Xenon lamp was positioned 15 cm away from the quartz reactor. Visible-light photocatalytic activities of prepared samples were evaluated by the photocatalysis of MB (40 ml of 10

mg/L) solution. The photocatalyst (0.15 g) was stirred to reach an adsorption-desorption equilibrium among the photocatalyst in the dark for 30 min. The MB concentration was determined by an UV-Vis spectrophotometer (UV-2550). 5 ml of the dye solution was taken out to measure the concentration change of MB after visible light irradiation for some time. When the 5 mL MB solution was taken out every 0.5 h, the xenon lamp was closed at the same time. After centrifugation, the absorbance of the dye was measured. Then, both the degradation liquid and the catalyst were re-added to the original reactor (the finally volume of the solution is still 40 mL). The xenon lamp was opened again. The photocatalytic degradation efficiency ( $E$ ) of MB was obtained by the following formula:  $E = (C_0 - C) / C_0 \times 100\% = (A_0 - A) / A_0 \times 100\%$ , where  $C$  is the concentration of the MB solution at reaction time  $t$ , and  $C_0$  is the adsorption-desorption equilibrium concentration of MB (at reaction time 0).  $A$  and  $A_0$  are the corresponding values of absorbance, respectively.

## Conclusion

In summary, Ag@AgCl/AgNbO<sub>3</sub> particles are successfully prepared by precipitation and photoreduction reaction. Partial Ag<sup>+</sup> ions of the AgCl particles were reduced to Ag<sup>0</sup> species under xenon light irradiation. Ag@AgCl/AgNbO<sub>3</sub> exhibits strong absorption in the whole visible-light region, and reveals much higher photocatalytic activity for the degradation of MB under visible-light irradiation than pure AgNbO<sub>3</sub> owing to surface plasmon resonance. The photoexcited electrons on the surface of the silver nanoparticles are injected and formed active species O<sub>2</sub><sup>-</sup>, HOO, H<sub>2</sub>O<sub>2</sub> and ·OH. The holes transfer to the surface of the AgCl particles to form Cl<sup>0</sup> atoms. Therefore, they can be used as efficient visible-light-induced material in wastewater treatment and air purification.

## Acknowledgements

The National Natural Science Foundation of China (No. 21302062) is gratefully acknowledged. The Science and technology developmental plan (No.201302060995F), and Science and Technology Development Plan of Jilin Province (No.20150101018JC) also supported this work.

## Notes and references

- 1 A. Kudo, K. Omori and H. Kato, *J. Am. Chem. Soc.*, 1999, **121**, 11459.
- 2 S. Tokunaga, H. Kato and, A. Kudo, *Chem. Mater.*, 2001, **13**, 4624.
- 3 M. Valant, A. Axelsson and N. Alford, *J. Eur. Ceram. Soc.*, 2007, **27**, 2549.
- 4 G. Q. Li, T. Kako, D. Wang, Z. Zou and J. Ye, *J. Solid State Chem.*, 2007, **180**, 2845.
- 5 D. Wang, T. Kako and J. Ye, *J. Am. Chem. Soc.*, 2008, **130**, 2724.
- 6 H. Kato, H. Kobayashi and A. Kudo, *J. Phys. Chem. B.*, 2002, **106**, 12441.
- 7 G. Li, S. Yan, Z. Wang, X. Wang and Z. Li, *Dalton Trans.*, 2009, **40**, 8519.

- 8 G. Li, T. Kako, D. Wang and Z. Zou, *Dalton Trans.*, 2009, **13**, 2423.
- 9 S. H. X. J and Li. H, *J. Alloys Compd.*, 2010, **496**, 633.
- 10 A. Veres, T. Rica, L. Janovak, M. Domok, N. Buzas, V. Zollmer, T. Seemann, A. Richardt and I. Dekany, *Catal. Today.*, 2012, **181**, 156.
- 11 M. Es-Souni, S. Habouti, N. Pfeiffer, A. Lahmar, M. Dietze and C. H. Solterbeck, *Adv. Funct. Mater.*, 2010, **20**, 377.
- 12 M. J. Uddin, F. Cesano, D. Scarano, F. Bonino, G. Agostini, G. Spoto, S. Bordiga and A. Zecchina, *J. Photochem. Photobiol. A-Chem.*, 2008, **199**, 64.
- 13 R. H. Wang, X. W. Wang and J. H. Xin, *ACS Appl. Mater. Interfaces.*, 2010, **2**, 82.
- 14 J. B. Zhou, Y. Cheng and J. G. Yu, *Journal of Photochemistry and Photobiology A: Chemistry.*, 2011, **223**, 82.
- 15 Z. J. Zhou, M. C. Long, W. M. Cai and J. Cai, *J. Mol. Catal. A-Chem.*, 2012, **353**, 22.
- 16 Q. J. Xiang, J. G. Yu, B. Cheng and H. C. Ong, *Chem. Asian J.*, 2010, **5**, 1466.
- 17 H. Zhang, X. F. Fan, X. Quan, S. Chen and H. T. Yu, *Environ. Sci. Technol.*, 2011, **45**, 5731.
- 18 J. J. Liu, Y. C. Yu, Z. X. Liu, S. L. Zuo and B. S. Li, *Int. J. Photoenergy.*, 2013, **6**, 728.
- 19 X. Zhou, C. Hu, X. Hu, T. Peng and J. Qu, *J. Phys. Chem. C.*, 2010, **114**, 2746.
- 20 J. Jiang and, L. Z. Zhang, *Chem. Eur. J.*, 2011, **17**, 3710.
- 21 P. Wang, B. B. Huang, X. Y. Zhang, X. Y. Qin, Y. Dai, Z. Y. Wang and Z. Z. Lou, *ChemCatChem.*, 2011, **3**, 360.
- 22 P. Wang, B. B. Huang, Z. Z. Lou, X. Y. Zhang, X. Y. Qin, Y. Dai, Z. K. Zheng and X. N. Wang, *Chem. Eur. J.*, 2010, **16**, 538.
- 23 P. Wang, B. B. Huang, X. Y. Zhang, X. Y. Qin, H. Jin, Y. Dai, Z. Y. Wang, J. W. Wei, J. Zhan, S. Y. Wang, J. P. Wang and W. B. Myung-Hwan, *Chem. Eur. J.*, 2009, 1821.
- 24 C. Wang, J. Yan, X. Y. Wu and H. M. Li, *Appl. Surf. Sci.*, 2013, **273**, 159.
- 25 M. Lukazewski., A. Kania. and A. Ratuszna, *J. Cryst. Growth*, 1980, **48**, 493
- 26 S. H. Feng, R. R. Xu, *Acc. Chem. Res.*, 2001, **34**, 239.
- 27 D. Wang, R. Yu, N. Kumada, N. Kinomura, *Chem. Mater.*, 2000, **12**, 956.
- 28 J. Yu, J. Xiong, B. Cheng and S. Liu, *Appl. Catal. B-Environ.*, 2005, **60**, 211.
- 29 D. L. Chen, S. H. Yoo, Q. S. Huang, G. Ali and S. O. Cho, *Chem. Eur. J.*, 2012, **18**, 5192.
- 30 H. Zhang, G. Wang, D. Chen, X. J. Lv and J. H. Li, *Chem. Mater.*, 2008, **20**, 6543.
- 31 T. Zhang, T. Oyama and A. Aoshima, *J. Photochem. Photobiol. A.*, 2001, **140(2)**, 163.
- 32 S. T. Gao, W. H. Liu, N. Z. Shang, C. Feng, Q. H. Wu, Z. W. and C. Wang, *RSC Adv.*, 2014, **4**, 61736.
- 33 Y. Y. Bu, Z. Y. Chen, C. Feng and W. B. Li, *RSC Adv.*, 2014, **4**, 38124.
- 34 H. B. Chang, M. H. Yuan and S. H. Feng., *J. Am. Ceram. Soc.*, 2012, **95**, 3408.
- 35 J. G. Yu, G. P. Dai and B. B. Huang, *J. Phys. Chem. C.*, 2009, **113**, 16394.